Please cite this article in press as: Kauts et al., *In Vitro* Differentiation of *Gata2* and *Ly6a* Reporter Embryonic Stem Cells Corresponds to *In Vivo* Waves of Hematopoietic Cell Generation, Stem Cell Reports (2017), https://doi.org/10.1016/j.stemcr.2017.11.018

Stem Cell Reports
**Article**

ISSCR

OPEN ACCESS

# *In Vitro* Differentiation of *Gata2* and *Ly6a* Reporter Embryonic Stem Cells Corresponds to *In Vivo* Waves of Hematopoietic Cell Generation

Mari-Liis Kauts,[1,2] Carmen Rodriguez-Seoane,[2] Polynikis Kaimakis,[1] Sandra C. Mendes,[1] Xabier Cortés-Lavaud,[2] Undine Hill,[1] and Elaine Dzierzak[1,2,*]

[1]Erasmus Medical Center Stem Cell Institute, Department of Cell Biology, Erasmus Medical Center, Rotterdam, the Netherlands
[2]Centre for Inflammation Research, Queens Medical Research Institute, University of Edinburgh, Edinburgh, UK
*Correspondence: elaine.dzierzak@ed.ac.uk
https://doi.org/10.1016/j.stemcr.2017.11.018

## SUMMARY

*In vivo* hematopoietic generation occurs in waves of primitive and definitive cell emergence. Differentiation cultures of pluripotent embryonic stem cells (ESCs) offer an accessible source of hematopoietic cells for blood-related research and therapeutic strategies. However, despite many approaches, it remains a goal to robustly generate hematopoietic progenitor and stem cells (HP/SCs) *in vitro* from ESCs. This is partly due to the inability to efficiently promote, enrich, and/or molecularly direct hematopoietic emergence. Here, we use *Gata2Venus* (*G2V*) and *Ly6a*(SCA1)*GFP* (*LG*) reporter ESCs, derived from well-characterized mouse models of HP/SC emergence, to show that during *in vitro* differentiation they report emergent waves of primitive hematopoietic progenitor cells (HPCs), definitive HPCs, and B-lymphoid cell potential. These results, facilitated by enrichment of single and double reporter cells with HPC properties, demonstrate that *in vitro* ESC differentiation approximates the waves of hematopoietic cell generation found *in vivo*, thus raising possibilities for enrichment of rare ESC-derived HP/SCs.

## INTRODUCTION

Since the first report of blood cell production from embryonic stem cells (ESCs) (Doetschman et al., 1985), it has been a long-term goal to use *in vitro* cultures to produce definitive hematopoietic progenitor cells (HPCs) and hematopoietic stem cells (HSCs). With the advent of patient-specific induced pluripotent stem cells (iPSCs), this approach could be used for treating blood disorders without the adverse effects of rejection. Some progress toward differentiation into distinct blood lineages has been made through addition of growth factors to ESC/iPSC differentiation cultures (Doulatov et al., 2013; Kennedy et al., 2012; Pearson et al., 2015), and limited *in vivo* repopulation has been achieved by overexpression of transcription factors in ESCs/iPSCs/endothelial cells (Lis et al., 2017; Sugimura et al., 2017). More fundamental studies on ESC hematopoietic differentiation have provided some insight into whether such *ex vivo* cultures recapitulate *in vivo* hematopoietic development (Choi et al., 1998; Huber et al., 2004; Lancrin et al., 2009).

The natural development of the hematopoietic system occurs in spatiotemporally distinct waves (reviewed in Dzierzak and Speck, 2008; Kauts et al., 2016). The first blood cell production occurs in the yolk sac (YS) at mouse embryonic day 7 (E7), producing a transient cell population of mainly primitive erythrocytes (Palis et al., 1999). Definitive erythrocytes and myeloid cells appear in the YS starting at E8.25 and originate from erythroid-myeloid progenitors (EMPs) (Frame et al., 2013). Shortly thereafter, HPCs with erythroid-myeloid-lymphoid potential (Godin et al., 1995), lymphoid progenitors (Boiers et al., 2013; Li et al., 2014), and neonatal-engrafting hematopoietic cells arise (Yoder et al., 1997). HSC production is initiated in the final wave starting at E10.5 in the aorta-gonads-mesonephros (AGM) (Medvinsky and Dzierzak, 1996; Muller et al., 1994).

The *Gata2* transcription factor plays a pivotal intrinsic role in EMP, HPC, and HSC generation in the embryo (de Pater et al., 2013; Gao et al., 2013; Ling et al., 2004; Tsai et al., 1994). *Gata2*$^{-/-}$ mouse and human (h) ESCs show defective hematopoietic differentiation (Huang et al., 2015; Tsai et al., 1994), and most hESC-derived HPCs are marked by GATA2 reporter expression, although it is uncertain whether this reporter parallels endogenous GATA2 expression (Huang et al., 2016). In our *Gata2Venus* (*G2V*) mice, in which levels of Gata2 expression are normal, it was found that Gata2 marks all HSCs and majority of HPCs. Gata2 is expressed in endothelial cells of the E8.5 YS and dorsal aorta (Minegishi et al., 1999; Robert-Moreno et al., 2005), E10.5 aortic hemogenic endothelial cells (HECs) (Eich et al., 2017), and C-KIT$^{+}$CD31$^{+}$ intra-aortic hematopoietic cluster cells (IAHCs) (Kaimakis et al., 2016). Thus, the *G2V* reporter facilitates the examination of HPCs and HSCs as they emerge in the mouse embryo. *Ly6a*(SCA1)*GFP* (*LG*) is another reporter that marks embryonic aortic cells. All HSCs, some HECs, IAHCs (Chen et al., 2011; de Bruijn et al., 2002; Li et al., 2014; Solaimani Kartalaei et al., 2015), and embryonic cells with lymphoid potential (de Bruijn et al., 2002; Li et al., 2014) are LG expressing. Vital imaging of the E10.5 mouse aorta shows endothelial-to-hematopoietic transition (EHT) of

Please cite this article in press as: Kauts et al., *In Vitro* Differentiation of *Gata2* and *Ly6a* Reporter Embryonic Stem Cells Corresponds to *In Vivo* Waves of Hematopoietic Cell Generation, Stem Cell Reports (2017), https://doi.org/10.1016/j.stemcr.2017.11.018

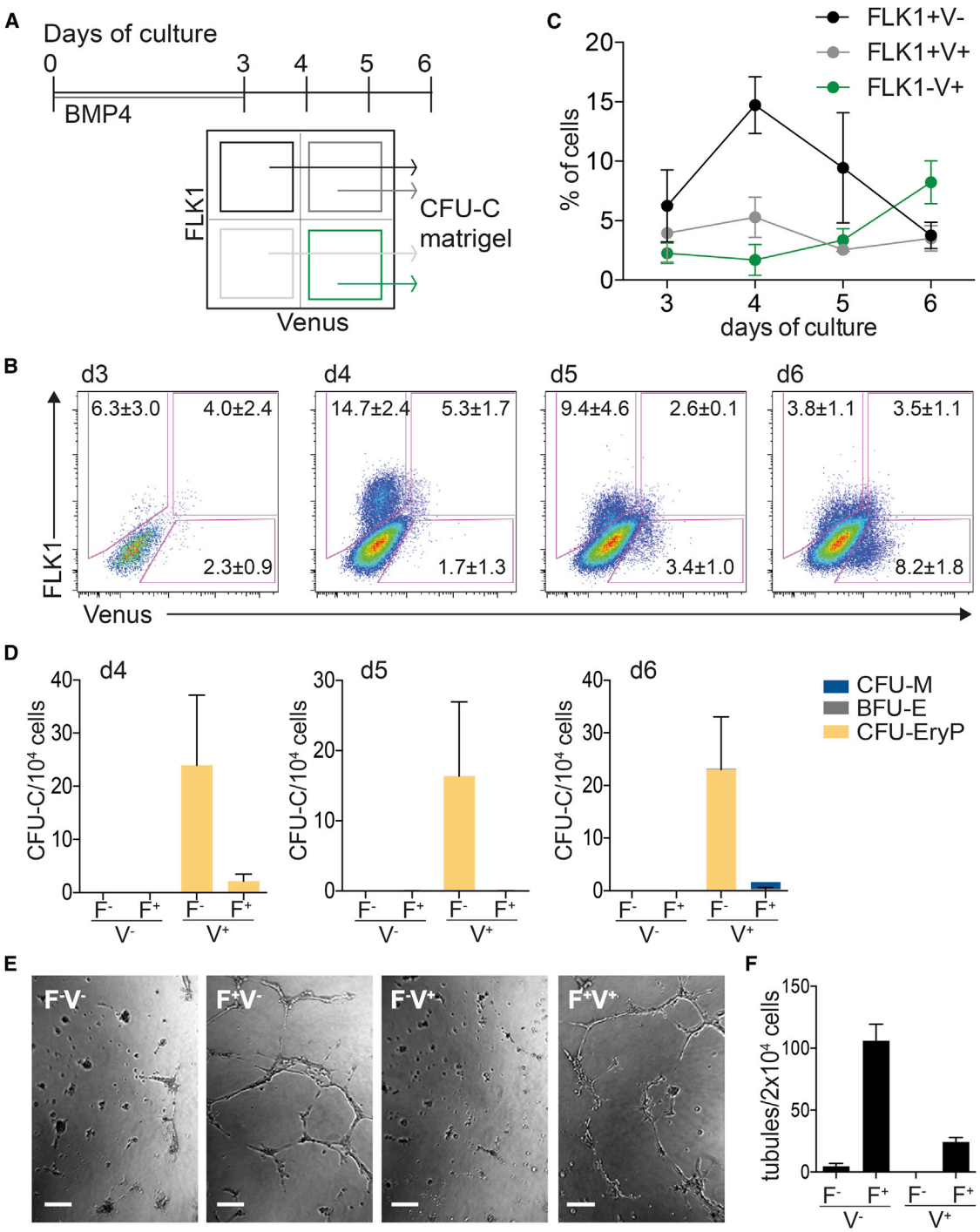


**Figure 1. G2V-Expressing Cells in Early Differentiation Culture Possess Primitive Erythroid and Endothelial Potential**

(A) Scheme of ESC differentiation. BMP4 was present on days 0–3. FACS-analyzed/sorted embryoid body (EB) cells were tested in CFU-C (colony-forming unit—cell) and Matrigel assays.

(B) Dot plots for FLK1 (F) and Venus (V) expression from day 3 (d3) to day 6 (n = 3).

(C) Quantification of FACS data in (B) showing percentage of $F^+V^-$, $F^+V^+$, and $F^-V^+$ cells at days 3–6 (n = 3).

(D) Bar graphs showing CFU-C/$10^4$ $F^+V^-$, $F^+V^+$, $F^-V^+$, and $F^-V^-$ cells at days 4–6 (n = 4). Colony types are indicated by color. CFU-M, macrophage; BFU-E, definitive erythroid; CFU-EryP, primitive erythroid.

*(legend continued on next page)*

these cells (Boisset et al., 2010). However, unlike the *G2V* reporter, $LG^+$ cells are found in the AGM only beginning at late E9 (Mascarenhas et al., 2009), and thus, this distinguishes the later induction of an intraembryonic definitive HPC/HSC program.

Taking into account the complex spatiotemporal organization of *in vivo* blood development, it is likely that the ability to robustly generate definitive HPC/HSC *in vitro* depends on the spatiotemporal programs occurring during ESC differentiation, and requires enrichment methodologies with pivotal reporters to identify/isolate the cells of interest. Such reporters are a powerful tool for studying the dynamics of functional HPC/HSC generation *in vitro* (Huber et al., 2004; Lancrin et al., 2009; Ng et al., 2016) and their relationship to normal HPC/HSC development.

Here we examine the expression of *G2V* and *LG* reporters and the emergence of functional hematopoietic cells in a stepwise *in vitro* system of induction, enrichment, and differentiation of ESCs. We show that the temporal wave-like *G2V* reporter expression corresponds to waves of primitive and definitive hematopoietic emergence. *Gata2* is co-expressed in these cells with hematopoietic transcription factors and marks functional HPCs emerging in the sequential waves. *LG* expression is specific to HPCs that emerge/persist in later differentiation stages, marking definitive progenitors with erythroid, myeloid, and/or B-lymphoid potential. This is confirmed in double reporter ESCs to show that *in vitro* differentiation occurs in stages that approximate the *in vivo* hematopoietic cell generation in mouse embryos.

## RESULTS

### Hematopoietic and Endothelial Potential of *Gata2*$^+$ ESCs

Hematopoiesis is initiated by $FLK1^+$ cells, which are able to generate endothelial and hematopoietic progenitors (Choi et al., 1998; Huber et al., 2004). In hESC differentiation cultures, $KDR^+$ cells develop in response to bone morphogenetic protein 4 (BMP4) between 72 and 96 hr and represent a transient population that precedes the onset of primitive hematopoiesis (Kennedy et al., 2007). To directly examine the relationship of *Gata2* expression and hematopoietic differentiation of mouse ESCs, we used a *G2V* reporter ESC line (Kaimakis et al., 2016) that facilitates tracing and isolation of live $Gata2^+$ cells by Venus fluorescence (Figure S1), while preserving normal Gata2 endogenous levels. This is critical, since altered Gata2 levels severely affect the production and expansion of embryonic HSCs and HPCs and affect HSC robustness in the adult (Ling et al., 2004; Rodrigues et al., 2005), and dysregulation leads to leukemic syndromes (Katsumura et al., 2017). To examine whether $Gata2^+$ cells possess endothelial or hematopoietic cell characteristics, we induced *G2V* ESC differentiation in the presence of BMP4 (Figure 1A) and analyzed them at days 3–6. $FLK1^+V^-$, $FLK1^-V^+$, $FLK1^+V^+$, and $FLK1^-V^-$ cells sorted by fluorescence-activated cell sorting (FACS) were evaluated in hematopoietic colony-forming unit—cell (CFU-C) and Matrigel endothelial assays.

At days 3 and 4, the majority of $V^+$ cells co-expressed FLK1 (67% and 76%, respectively) (Figure 1B). As the $FLK1^+V^+$ cell frequency decreased at day 5, the $V^+$ single positive population became more prominent and $FLK1^+$ cell frequency decreased (Figure 1C). Only the $V^+$ fraction produced CFU-C (Figure 1D). CFU-Cs were detected from day 4 onward, with the main colony type being CFU-EryP (—primitive erythroid). Few CFU-M (—macrophages) and burst-forming units—definitive erythroid (BFU-E) progenitors were observed. Although the majority of colonies were scored in the $FLK1^-V^+$ population ($24 \pm 13$, $16 \pm 11$, and $23.2 \pm 10$ CFU-C/$10^4$ cells at days 4, 5, and 6, respectively), CFU-C were also detected in the $FLK1^+V^+$ cells at day 4.

To test the day-4 endothelial potential of ESCs (time of highest CFU-C potential in $FLK1^+V^+$ fraction), we quantified tubule formation of sorted cells (Figures 1E and 1F). The highest frequency was in $FLK1^+V^-$ cells (100 tubules/$2 \times 10^4$ cells). $FLK1^+V^+$ cells also showed endothelial potential (30 tubules/$2 \times 10^4$ cells), demonstrating that in addition to hematopoietic potential, some $FLK1^+V^+$ cells are capable of endothelial differentiation. This transient Gata2-expressing $FLK1^+$ population emerges at day 4 and rapidly decreases thereafter. Thus, Gata2-expressing $FLK1^+$ cells give rise to the earliest blood cells.

### Temporally Defined *Gata2* Expression Waves Are Detected in ESC Cultures

The temporal dynamics of Gata2 expression was characterized in ESC hematopoietic differentiation from days 4 to 14 by FACS (Figures 2 and S1D). $V^+$ cells were detected throughout the time course and showed wave-like dynamics with peaks of increased $V^+$ cell frequency. Compared with day 4, day-6 $V^+$ cell percentages were significantly higher (5.5-fold) (Figure 2A) and then

(E) Representative images showing endothelial tubules in Matrigel cultures of $F^+V^-$, $F^+V^+$, $F^-V^+$, and $F^-V^-$ cells from day-4 differentiated ESCs. Scale bars, 200 μm.
(F) Quantification of (E) (tubules/$2 \times 10^4$ cells; n = 3).
Data are shown as means ± SEM. See also Figure S1.

Please cite this article in press as: Kauts et al., *In Vitro* Differentiation of *Gata2* and *Ly6a* Reporter Embryonic Stem Cells Corresponds to *In Vivo* Waves of Hematopoietic Cell Generation, Stem Cell Reports (2017), https://doi.org/10.1016/j.stemcr.2017.11.018

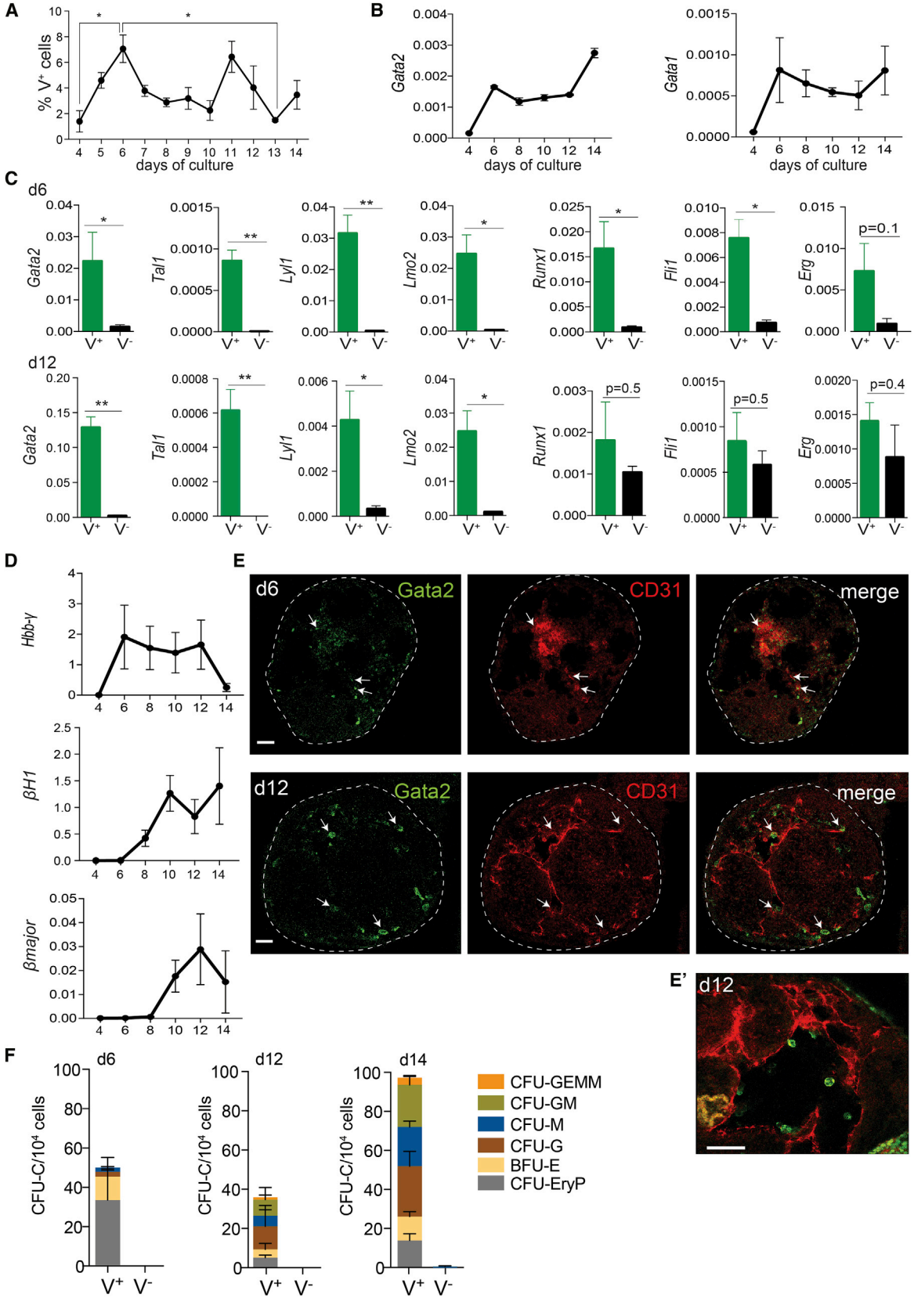


*(legend on next page)*

decreased at days 7–10. $V^+$ cell percentages increased again at day 11, decreased at day 13, and increased again at day 14 (RNA analysis in Figure S1E). *Gata2* RNA expression (Figure 2B) showed increases at days 6 and 14 that correspond with the $V^+$ cell frequency (Figure 2A; no *Gata2* RNA analysis performed at day 11). To exclude the possibility that the later *Gata2* expression peaks are due to the remaining undifferentiated ESCs, we analyzed the expression of the Nanog pluripotency factor. *Nanog* RNA was significantly decreased after day 3 of differentiation and no protein was detected at d12 (Figures S1F and S1G). Also, *Brachyury* expression, indicative of primitive streak/mesoderm, showed the expected dynamics with increased expression at days 3–6, and was downregulated thereafter (Figure S1H), thus supporting the likelihood of independent induction waves of *Gata2*$^+$ hematopoietic cells in ESC cultures.

*Gata2* functions in combination with other key (heptad) hematopoietic transcription factors to direct HPC/HSC development (Wilson et al., 2010). The expression of *Gata2*, *Tal1*, *Lyl1*, *Lmo2*, *Fli1*, *Runx1*, and *Erg* was tested (by qRT-PCR) in $V^+$ and $V^-$ sorted cells (Figure 2C). *Gata2*, *Tal1*, *Lyl1*, *Lmo2*, *Runx1*, and *Fli1* were significantly higher in the day-6 $V^+$ compared with $V^-$ cells. At day 12, *Gata2*, *Tal1*, *Lyl1*, and *Lmo2* were significantly higher in $V^+$ compared with $V^-$ cells. Similar expression levels of *Erg* were found in $V^+$ and $V^-$ cells at day 6/day 12, and *Runx1* and *Fli1* expression levels in these fractions were similar at day 12. As a control, the expression of a non-heptad ubiquitous transcription factor, *Cbfβ* (Runx1 binding partner), was assessed (Figure S1I) and found to be similarly expressed in day-6 $V^+$ and $V^-$ cells. Thus, the expression of the relevant heptad hematopoietic transcription factors in ESC-derived Gata2$^+$ cells indicates a developmental hematopoietic gene expression profile consistent with that found in mouse embryos (Eich et al., 2017).

## Sequential Waves of *Gata2*$^+$ Cells Correlate with Functional Primitive and Definitive Hematopoietic Potential

Hematopoiesis in the mouse embryo occurs in stage-specific waves, with the generation of cells with progressively greater multipotent hematopoietic properties. To elucidate whether $V^+$ cells in the sequential waves express genes indicative of primitive (*Hbb-y* and *βH1*; early erythroid) and/or definitive (*βmajor*; adult erythroid) programs (Palis et al., 2010; Sankaran et al., 2010), we performed qRT-PCR (Figure 2D). *Gata1* (pan-erythroid factor) showed expression at days 6 to 14 (Figure 2B, right). *Hbb-y* was expressed from days 6 to 12 and decreased at day 14 (Figure 2D, upper), and *βH1* expression was detected from day 8 onward (Figure 2D, middle). Expression of both embryonic globins preceded the onset of *βmajor* (adult globin) expression that was detectable from day 10 onward (Figure 2D, lower), suggestive of definitive erythropoiesis.

In the mouse embryo, CD31$^+$ HPCs/HSCs emerge from CD31$^+$ HECs (Boisset et al., 2010; Yokomizo et al., 2012). CD31$^+$, $V^+$, and CD31$^+$V$^+$ cells were detected in day-6 and day-12 embryoid bodies (EBs) (Figures 2E and 2E′). The morphology and localization of $V^+$ cells in CD31 immunostained whole EBs was analyzed by confocal microscopy. At day 6, CD31$^+$ cells were dispersed throughout the EBs with no distinct structural organization, and flat endothelial-like V$^+$CD31$^+$ cells were found (Figure 2E). At day 12, round hematopoietic-like V$^+$CD31$^+$ cells were closely associated with the CD31$^+$ cells lining the EB cavities (Figures 2E [lower] and 2E′). These imaging data indicate that $V^+$ cells in the day-6 and day-12 EBs are morphologically distinct, and thus may possess different functions.

To test the relationship between *Gata2* expression, stage of differentiation, and hematopoietic function, we harvested cells from day-6, -12, and -14 EBs, sorted $V^+$ and

**Figure 2. G2V Temporal Expression Defines Primitive and Definitive Hematopoietic Stages of ESC Differentiation**

(A) Percentage of Venus$^+$ ($V^+$) cells in day 4–14 *G2V* ESC cultures (n = 3).

(B) Relative *Gata2* (left) and *Gata1* (right) *mRNA* as measured in qRT-PCR analysis of differentiated (total unsorted) cells from *G2V* ESC at days 4, 6, 8, 10, 12, and 14. Normalization to *β-actin* (n = 3).

(C) Relative *Gata2*, *Tal1*, *Lyl1*, *Lmo2*, *Runx1*, *Fli1*, and *Erg mRNA* as measured in qRT-PCR analysis of $V^+$ and $V^-$ cells at days 6 (upper) and 12 (lower) of *G2V* ESC culture. Normalization to *β-actin* (n = 3).

(D) qRT-PCR analysis of relative *Hbb-y* (*embryonic globin*), *βH1* (*embryonic globin*), and *βmajor* (adult globin) *mRNA* of cells from *G2V* differentiated ESCs at days 4, 6, 8, 10, 12, and 14. Normalization to *β-actin* (n = 3).

(E) Confocal images (representative) of whole-mount stained day-6 (upper) and day-12 (lower) EBs. Venus, green; CD31, red. Arrows indicate flat endothelial-like $V^+$ cells in day-6 EBs and round hematopoietic-like $V^+$ cells/clusters in day-12 EBs. Scale bars, 40 μm. (E′) Magnification of whole-mount stained day-12 EB showing round $V^+$ cells within the EB cavity close to CD31$^+$ endothelial cells. Scale bar, 40 μm.

(F) Bar graphs showing CFU-C per $10^4$ $V^+$ and $V^-$ cells from day-6 and day-12 *G2V* ESCs (n = 3). CFU-GEMM, granulocyte-erythrocyte, monocyte-macrophage; CFU-GM, granulocyte-macrophage; CFU-M, macrophage; CFU-G, granulocyte; BFU-E, definitive erythroid; CFU-EryP, primitive erythroid.

Data are shown as means ± SEM. *$p < 0.05$, **$p < 0.01$. See also Figures S1 and S2.

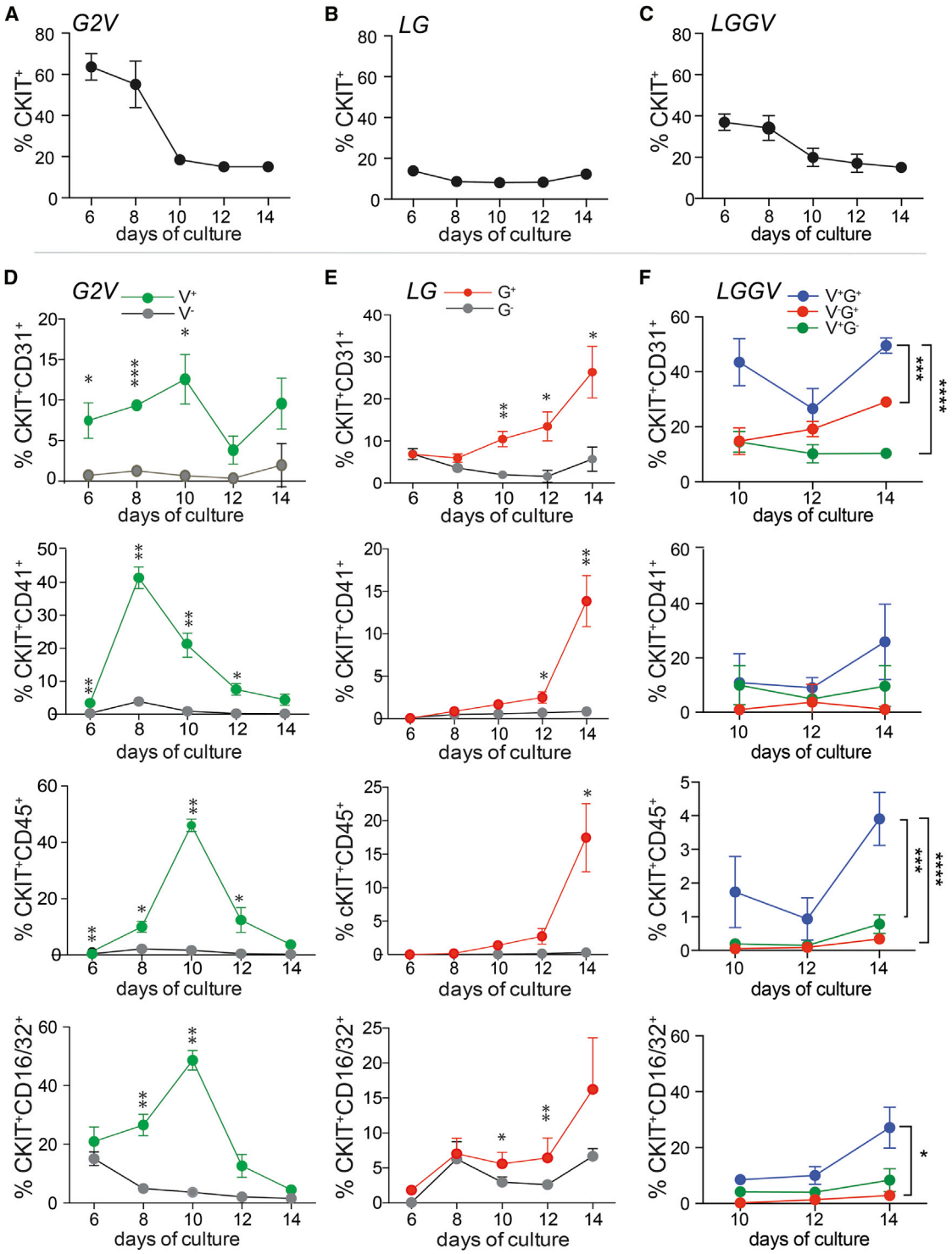


**Figure 3. Temporal Phenotypic Analysis of Reporter ESC-Derived Cells during Hematopoietic Differentiation**

(A–C) Percentage of C-KIT$^+$ cells in total viable cells from differentiated (A) *G2V* (n = 6), (B) *LG* (n = 3), and (C) *LGGV* (day 6, n = 3; day 8 and day 12, n = 4; day 10, n = 7; day 14, n = 5) ESCs at days 6, 8, 10, 12, and 14.

(D and E) Graphs showing the percentage of C-KIT$^+$CD31$^+$, C-KIT$^+$CD41$^+$, C-KIT$^+$CD45$^+$, and C-KIT$^+$CD16/32$^+$ cells in the reporter$^+$ and reporter$^-$ cells at days 6, 8, 10, 12, and 14. (D) *G2V* (V$^+$, green; V$^-$, black; n = 3); (E) *LG* ESCs (G$^+$, red; G$^-$, black; n = 4).

*(legend continued on next page)*

$V^-$ cells, and analyzed CFU-C. HPCs were found exclusively in the $V^+$ cell fractions (Figure 2F). Day-6 $V^+$ cells gave rise to 50.1 ± 13 CFU-C/$10^4$ cells (1 HPC:198 cells), whereas day-12 $V^+$ cells generated 36.0 ± 25 (1:278) and day-14 $V^+$ cells 94.7 ± 20 CFU-C/$10^4$ cells (1:278). The majority (67%) of day-6 cells had CFU-EryP potential. Only a low frequency of macrophage, granulocyte, and definitive erythroid (CFU-M, CFU-G, BFU-E) colonies were observed. In contrast, day-12 and day-14 cells gave rise to a variety of erythroid-myeloid colony types, including mixed multipotent colonies (CFU-GEMM), suggesting that day-12, but not day-6 $V^+$ cells possess EMP potential. Moreover, the day-14 progenitor frequency was increased 2.6-fold compared with day 12, and more mixed multipotent colonies were detected (Figure 2F). CFU-C derived from day-12 to -14 progenitors exhibited significantly increased proliferation capacity compared with the CFU-C from day-6 EBs. Together these data indicate that $Gata2^+$ cells represent at least two different stages of induction in ESC cultures that correlate with primitive and erythroid-myeloid definitive functional cell potentials and molecular programs.

## Gata2-Expressing C-KIT$^+$ Cells Show Phenotypic Markers Characteristic of Definitive Hematopoiesis

*G2V* ESCs were examined for C-KIT expression (marker of cells undergoing transition to the hematopoietic lineage) during the ESC differentiation culture. A high frequency of C-KIT$^+$ cells was found at day 6 (~64%) and decreased to ~16% by days 10–14 (Figure 3A). The co-expression of C-KIT with CD31 (endothelial and hematopoietic marker), CD41 (HPC and megakaryocyte marker), CD45 (pan-hematopoietic), and CD16/32 (EMP marker co-expressed with C-KIT) was measured together with Venus expression on differentiated cells by FACS (Figures 3D and S3). CD31$^+$C-KIT$^+$ cells were detected predominantly in $V^+$ fraction, whereas very few $V^-$ cells showed this phenotype. The percentages of CD31$^+$C-KIT$^+$ cells in the $V^+$ fraction increased steadily at days 6–10, with a low point at day 12, and then rose again, suggesting a late wave of hematopoietic emergence. Four percent of day-6 $V^+$C-KIT$^+$ cells were CD41$^+$ and this increased to 41% ± 3.3% at day 8, followed by decreases at days 10–14. Interestingly, C-KIT was mainly detected on $V^+CD41^{lo}$ and not $V^+CD41^{hi}$ cells, in line with published data showing that AGM HP/SCs express CD41 at low/intermediate levels (Robin et al., 2011). Very few $V^-$ cells were CD41$^+$ throughout all time points analyzed, thus suggesting that co-expression of Gata2, $CD41^{lo}$, and C-KIT define an HP/SC population during ESC differentiation. CD45 expression was barely detectable in $V^+$C-KIT$^+$ cells at day 6 (1.3%). There was a profound increase and peak at day 10 with 46% ± 2.2% of $V^+$ cells CD45$^+$C-KIT$^+$ (as compared with the peak of CD41$^+$C-KIT$^+$ cells at day 8), and this was followed by decreased CD45$^+$C-KIT$^+$ cell percentages at days 12 and 14. No to very few $V^-$ cells were CD45$^+$C-KIT$^+$ (0.4%–2.2%) throughout the differentiation. Thus, CD45 is confirmed as a later marker of hematopoietic cells. EMP markers CD16/32 were highly expressed at day 10. Eighty-five percent of day-10 $V^+$C-KIT$^+$ cells were CD16/32$^+$, suggesting that the erythroid-myeloid CFU-C potential detected in the culture at days 12–14 emerges from CD16/32$^+V^+$ EMPs. In contrast to the other markers, CD16/32 was expressed also in $V^-$ cells (15% ± 2.3% and 21% ± 5.0% at day 6). This is expected and is in line with the *in vivo* results showing *Gata2*-independent EMPs (Kaimakis et al., 2016). When the viability of day-10 to -14 $V^+$ cells was tested (Figure S1J) no profound change in cell viability was found, indicating that the decreased frequency in phenotypic HPCs is not related to cell death. Together, these data demonstrate that Gata2 expression defines most phenotypic HPCs generated throughout ESC differentiation (both early and later) and that these markers reveal wave-like cell kinetics.

## The *LG* Reporter Distinguishes a Late Hematopoietic Wave with Multilineage Potential

Unlike *G2V* reporter embryos in which Gata2 expression marks almost all hematopoietic cells from the earliest time of generation, the SCA1 (*LG*) reporter *in vivo* is expressed in fewer hematopoietic cells and in cells generated at later developmental stages (Boisset et al., 2010; de Bruijn et al., 2002). Analysis of day-10 and day-14 *G2V* ESC cultures showed respectively that 3.7% and 2.2% of cells expressed SCA1 (Figure 4A). Of the day-10 SCA1$^+$ cells, less than 1% were C-KIT$^+$CD45$^+$. Although a slightly higher percentage of SCA1$^+$ cells was found in day-10 cultures, the day-14 cultures contained a 6-fold higher percentage of C-KIT$^+$CD45$^+$ cells in the SCA1$^+$ fraction, indicating that the *LG* reporter may be a relevant tool to aid enrichment for hematopoietic progenitors late in ESC differentiation cultures.

An *LG* ESC line was established from the *LG* mouse model to examine reporter expression kinetics during ESC differentiation. FACS analysis (Figure 4B) showed the presence of GFP$^+$ (G$^+$) cells already at days 3 (7%) and 4

(F) Graphs showing the percentage of C-KIT$^+$CD31$^+$, C-KIT$^+$CD41$^+$, C-KIT$^+$CD45$^+$ and C-KIT$^+$CD16/32$^+$ cells in $V^+G^+$ (blue), $V^-G^+$ (red), and $V^+G^-$ (green) cell fractions of *LGGV* ESCs at days 10, 12, and 14 (n > 3).

Data are shown as means ± SEM. Significant differences between reporter$^+$ and reporter$^-$ frequencies are indicated. *p < 0.05, **p < 0.01, ***p < 0.001, ****p < 0.0001. See also Figures S3, S4, S6, and S7.

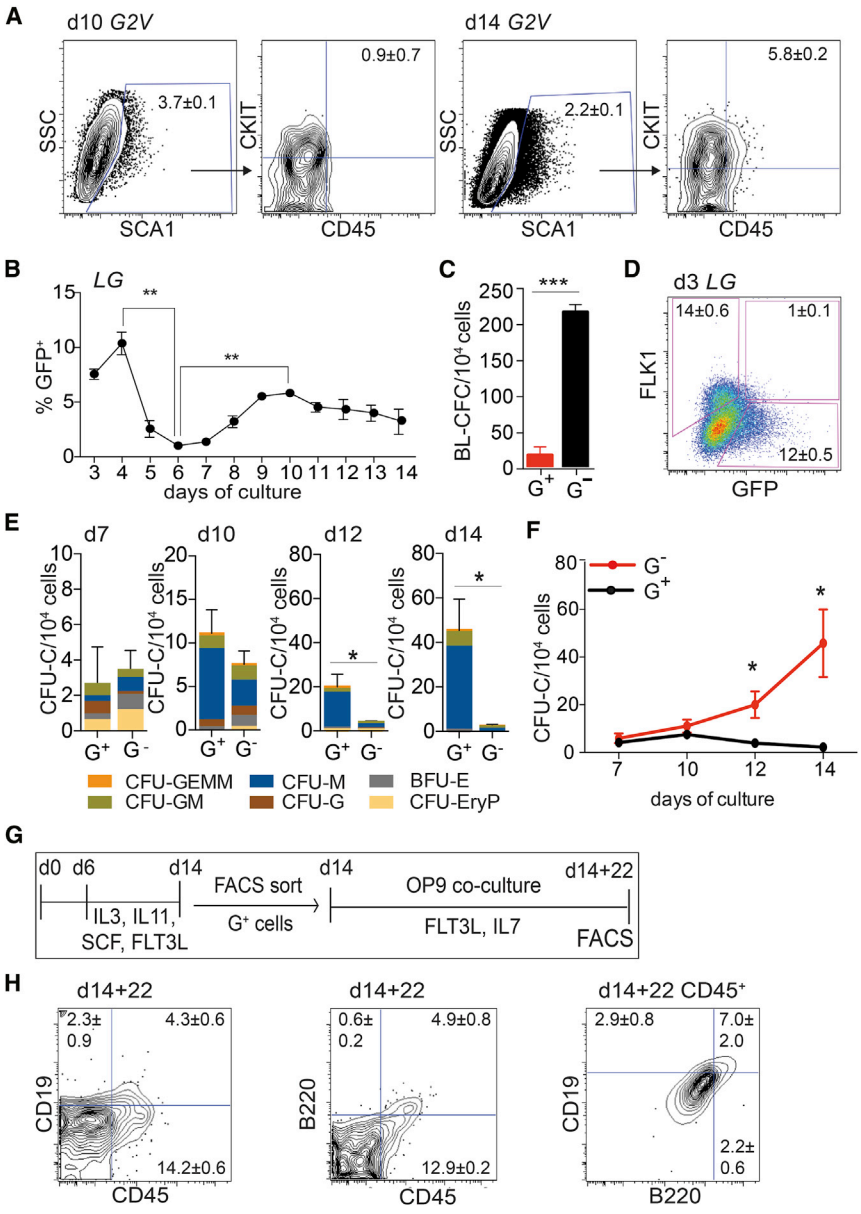


**Figure 4. LG Expression Distinguishes Functional Hematopoietic Cells in the Definitive ESC Differentiation Stage**

(A) FACS analysis of day-10 and day-14 *G2V* ESC for SCA1$^+$ cells. Percentages of SCA1$^+$ and SCA1$^+$C-KIT$^+$CD45$^+$ cells are indicated (n = 3).

(B) Percentage of G$^+$ cells in cultures of differentiated *LG* ESCs at days 4–14 (n = 3).

(C) Blast colony (BL-CFC) potential in G$^+$ and G$^-$ cells sorted from day-3 *LG* ESCs (n = 3).

(D) FACS dot plot showing percentage of cells expressing FLK1 and/or GFP in day-3 *LG* ESC cultures (n = 3).

(E) CFU-C potential of G$^+$ and G$^-$ cells from *LG* ESC cultures harvested at days 7, 10, 12, and 14 (CFU-C/10$^4$; n = 4). Colony types correspond to color code. CFU-GEMM, granulocyte, erythrocyte, monocyte, macrophage; CFU-GM, granulocyte-macrophage; CFU-M, macrophage; CFU-G, granulocyte; BFU-E, definitive erythroid; CFU-EryP, primitive erythroid.

(F) Time course of CFU-C frequency in cultures of *LG* ESC-derived G$^+$ (red) and G$^-$ (black) cells at days 7, 10, 12, and 14. Significant differences between CFU-C/10$^4$ G$^+$ and G$^-$ cells are indicated (n = 4).

(G) Lymphoid culture protocol used for differentiation and enrichment of G$^+$ cells from *LG* ESCs.

(H) B-lymphoid marker CD19 and B220 FACS of day-14 + day-22 CD45$^+$ cells and CD19$^+$B220$^+$ (gated CD45$^+$) cells from *LG* lymphoid differentiation cultures.

Data are shown as means ± SEM. *p < 0.05, **p < 0.01, ***p < 0.001. See Figure S5 for percentage (n = 5) and controls.

(10%), followed by a rapid 5-fold decrease. G$^+$ cell percentages increased at day 7 and peaked at days 9–10 of differentiation (3-fold increase; 6% at day 10).

The percentage of C-KIT$^+$ cells in cultures at days 6–14 averaged ~17% with little change (Figure 3B), indicating less efficient hematopoietic differentiation of the *LG* line compared with *G2V* line (Figure 3A). Next, C-KIT and co-expression of CD31, CD41, CD45, and CD16/32 within the G$^+$ and G$^-$ fractions of day-6 to -14 *LG* ESC cultures was determined (Figures 3E and S4). At day 6 the percentages of CD31$^+$C-KIT$^+$ cells in G$^+$ and G$^-$ fractions, respectively (6.9% ± 0.4% and 6.9% ± 1.3%), were similar. From day 10 onward, the percentage of CD31$^+$C-KIT$^+$ cells increased in the G$^+$ (rising to 26.0% ± 6.2%) compared with the G$^-$ fraction. CD41$^+$C-KIT$^+$ cells were detected beginning at day 8 in G$^+$ cells (0.9% ± 0.2%) and gradually increased to 14% ± 3.0% at day 14. Percentages of CD45$^+$C-KIT$^+$ showed a trend similar to that of CD41$^+$C-KIT$^+$ cells and were detected in the G$^+$ fraction from day 8 (0.2% ± 0.1%) onward. The frequency increased significantly after day 12 and rose to 18% ± 5.1% at day 14. The G$^-$ fraction contained no to very few CD45$^+$C-KIT$^+$ cells. C-KIT$^+$CD16/32$^+$ cells were detected from day 8 onward in both G$^+$ and G$^-$ fractions, with the frequency of C-KIT$^+$CD16/32$^+$ cells increasing considerably in the G$^+$ fraction at days 10–12. These data indicate that *LG* reports

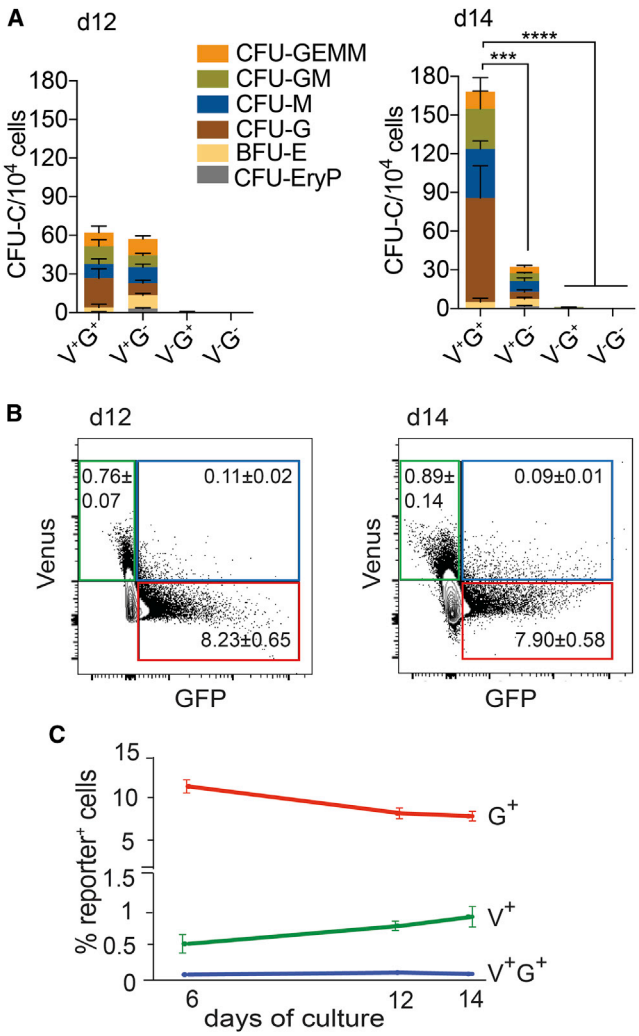


**Figure 5. Late-Stage *LGGV* ESC Differentiation Cultures Contain a High Frequency of HPCs in the Double Reporter-Positive Population**

(A) CFU-C/$10^4$ cells in day-12 (left; n = 6) and day-14 (right; n = 6) $V^+G^+$, $V^+G^-$, $V^-G^+$, and $V^-G^-$ fractions of differentiated *LGGV* ESCs. Color code indicates colony type.

(B) FACS plots of viable reporter$^+$ cells in day-12 (n = 8) and day-14 (n = 10) *LGGV* ESC differentiation cultures. Gated $V^+$ (green), $G^+$ (red), and $V^+G^+$ (blue) cells.

(C) Percentage of $V^+$ (green), $G^+$ (red), and $V^+G^+$ (blue) cells in the total viable cells on days 6, 12, and 14 of *LGGV* ESC differentiation. Data are shown as means ± SEM. ***p < 0.001, ****p < 0.0001. See also Figure S6.

phenotypic hematopoietic cells predominantly in the later stages of ESC differentiation.

The relationship of GFP expression with hematopoietic activity in the *LG* ESC culture was tested by blast colony-forming assay. At early differentiation stages (day 3), significantly more blast colonies (BL-CFC) per $10^4$ cells were found in the $G^-$ fraction (215 ± 11) than in the $G^+$ fraction (17 ± 12) (Figure 4C). Accordingly, very few $FLK1^+G^+$ cells were found (1% ± 0.1%) (Figure 4D). CFU-C assays from day-7 EBs revealed a small number of HPCs in both $G^+$ and $G^-$ fractions (Figure 4E). However, at days 12 and 14 significantly more CFU-Cs, including all the CFU-GEMMs, were found in the $G^+$ fraction. CFU-C frequencies increased from day 7 to day 14 (Figures 4E and 4F) but were similar in the $G^+$ and $G^-$ fractions at days 7 and 10. A significantly higher frequency of CFU-C was in the $G^+$ fraction than the $G^-$ fraction at day 12, and at day 14 virtually all CFU-Cs were in the $G^+$ fraction. This 2.3-fold increase in CFU-C frequency from day 12 to ay 14 indicates that the LG reporter enriches for late appearing HPCs.

To examine whether late appearing cells have B-lymphoid potential, we co-cultured day-14 *LG* EB-derived $G^+$ cells for 22 days on OP-9 cells with lymphoid-promoting factors (Figure 4G). FACS analysis of B cell markers CD19 and B220 revealed that 4.3% ± 0.6% of the cells were $CD19^+CD45^+$ and 4.9% ± 0.8% were $B220^+CD45^+$. Seven percent of $CD45^+$ were positive for both CD19 and B220 (Figures 4H and S5). Thus, some *LG* reporter-expressing cells possess B-lymphoid potential.

## Double Reporter Expression Defines Most HPCs in Late-Stage ESC Differentiation

To assess whether *G2V* and *LG* reporter expression is overlapping, we established a *Ly6a*(SCA1)*GFP*:*Gata2Venus* (*LGGV*) double ESC reporter line and examined the kinetics and frequency of reporter-expressing hematopoietic cells during differentiation (Figures S6, 5B, and 5C).

The efficiency of *LGGV* ESC hematopoietic differentiation was determined by C-KIT FACS analysis at days 6, 8, 10, 12, and 14 (Figure 3C). The percentage of $C\text{-}KIT^+$ cells in the total viable cell population of day-6 and -8 *LGGV* cultures was 37% and 34% respectively. At days 10–14, the cultures contained an average of 18% $C\text{-}KIT^+$, thus indicating that the temporal hematopoietic differentiation efficiency of the *LGGV* line is similar to that of the *G2V* line (Figure 3A). Next, analysis for co-expression of C-KIT and CD31, CD41, CD45, or CD16/32 within the $V^+G^+$, $V^+G^-$, and $V^-G^+$ fractions of day-10, -12, and -14 ESC differentiation cultures was performed (Figures 3F and S7). In general, the highest percentage of $C\text{-}KIT^+CD31^+$, $C\text{-}KIT^+CD41^+$, $C\text{-}KIT^+CD45^+$, and $C\text{-}KIT^+CD16/32^+$ cells was in the $V^+G^+$ fraction at all three time points. Moreover, at day 14 for all the markers except for $C\text{-}KIT^+CD41^+$, significant increases in the percentages of marker-positive cells were found in the $V^+G^+$ fraction as compared with the $V^+G^-$ and/or $V^-G^+$ fractions, indicating a late shift in phenotypic hematopoietic progenitors.

To determine in which reporter-expressing populations HPC function was localized, we differentiated

Please cite this article in press as: Kauts et al., *In Vitro* Differentiation of *Gata2* and *Ly6a* Reporter Embryonic Stem Cells Corresponds to *In Vivo* Waves of Hematopoietic Cell Generation, Stem Cell Reports (2017), https://doi.org/10.1016/j.stemcr.2017.11.018

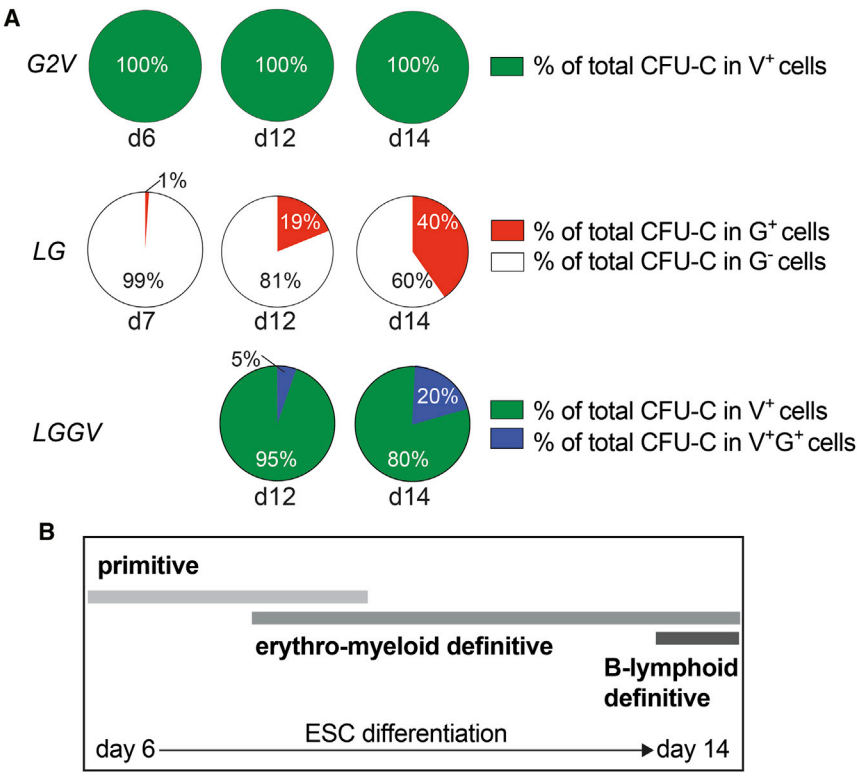


**Figure 6. Temporal Distribution of Hematopoietic Progenitors in Reporter ESC Differentiation Cultures**

(A) Percentage of CFU-C/$10^4$ cells in day-6, -12, and -14 differentiated *G2V* ESC-derived $V^+$ cells (green) (upper); in day-7, -12, and -14 differentiated *LG* ESC-derived $G^+$ (red) and $G^-$ cells (white) (middle); and in day-12 and -14 differentiated *LGGV* ESC-derived $V^+G^+$ (blue) and $V^+$ cells (green) (lower). CFU-C frequencies are calculated based on the percentage of respective reporter-expressing cells in the total population.

(B) Time-course model showing waves of primitive, erythroid-myeloid-definitive, and B-lymphoid-definitive hematopoietic progenitor activities in multireporter ESC differentiation cultures.

*LGGV* ESCs, and analyzed day-12 and day-14 single ($V^+G^-$ and $V^-G^+$) and double ($V^+G^+$) reporter-expressing cells along with reporter-negative ($V^-G^-$) cells (Figure 5A). At day 12, 119 CFU-C/$10^4$ were detected, of which 57 were derived from $V^+G^-$ and 62 from $V^+G^+$ fractions. Negligible to no CFU-Cs were present in the $V^-G^+$ or $V^-G^-$ fractions. The CFU-C frequency at day 14 increased to 200/$10^4$ cells, and all CFU-GEMM were in the $V^+G^+$ fraction (Figure 5A). Interestingly, when taking into account the frequency of reporter-expressing cells in the total cell population derived from *LGGV* EBs (Figures 5A and 5B), overall CFU-C frequency in the day-14 $V^+G^+$ versus $V^+G^-$ fraction increased 4-fold (from 5% to 20% of the total colonies) compared with day 12 (Figure 6A, lower). This is in line with the increase in CFU-C frequency in the $G^+$ versus $G^-$ fractions derived from day-12 and day-14 *LG* cultures (Figure 6A, middle). Colonies derived from *G2V* cultures were found only within the $V^+$ fraction throughout differentiation (Figure 6A, upper).

Together, these data suggest that a subset of progenitors is generated and/or gradually acquires the LG marker later in the culture and possesses more complex hematopoietic potential, thereby distinguishing and allowing specific enrichment of a more potent definitive wave of ESC hematopoietic emergence.

## DISCUSSION

In this study, we show that ESC differentiation progresses through stages of functional hematopoietic cell production that can be discriminated by the *G2V* and/or *LG* reporters (Figure 6B). The fact that these reporters are validated *in vivo* indicators of normal temporal and spatial generation of functional hematopoietic cells in the mouse embryo (de Bruijn et al., 2002; Kaimakis et al., 2016; Li et al., 2014; Solaimani Kartalaei et al., 2015) ensures high fidelity in their use to examine the stages of hematopoietic emergence *in vitro*. The reporter-expressing ESC-derived cells exhibit functional hematopoietic properties that correspond to cells generated in the *in vivo* waves of hematopoietic emergence.

Hematopoiesis in the mouse embryo starts in the YS with a transient wave of primitive hematopoiesis, and is characterized by $FLK1^+$ cells that give rise to the earliest blood cells and endothelium (Choi et al., 1998; Kennedy et al., 1997; Palis et al., 1999; Shalaby et al., 1997). Our analysis of early *G2V* EB differentiation (days 4–6) reveals a transient $FLK1^+V^+$ population that differentiates into endothelial and/or primitive erythroid cells. In contrast, early *LG* EB differentiation shows that most FLK1 expression is in the $G^-$ cell fraction and blast colony-forming activity is in the $FLK^+$ and $G^-$ cell fraction. Thus, *G2V* but not *LG* reports the earliest onset of hematopoietic potential in ESCs.

$V^+$ cells, albeit very few, are already present at day 4 of *G2V* ESC differentiation. It was difficult to detect *Gata2*, *Gata1*, and globin gene expression at day 4 (Figure 2B) by qRT-PCR of total *G2V* EB RNA. Others have shown, by single cell transcriptomics performed on pseudotemporally ordered E7.5–7.75 $FLK1^+$ mesodermal cells, an upregulation of *Gata1*, *βH1*, and *Itga2b* (CD41) following *Brachyury* expression during primitive streak specification (Scialdone et al., 2016). In total EB RNA, we found *Brachyury* expression at days 3 and 6 (Figure S1H), indicating that at least some differentiating EBs closely follow the formation of early mesoderm in gastrulating embryos. *Gata1* and *Gata2* expression was initiated at days 4–6. Embryonic globin *Hbby* and *βH1* expression began at days 4–6 and 6–8, respectively, and adult globin (*βmajor*) expression began at days 8–10 (Figure 2D) although its levels were relatively low. These data are somewhat in agreement with those found in the mouse embryo (Sankaran et al., 2010). *βH1* expression begins in the YS at E7.5 (Kingsley et al., 2006), with only very low levels of *Hbby* and *βmajor* expression. *Hbby* expression is high in the E10.5 and E15.5 peripheral blood, and *βmajor* expression is high in the enucleated E15.5 erythrocytes. Thus, while the general onset of expression of the embryonic globins prior to *βmajor* expression is similar to *in vivo* expression, the other differences seen in the ESC differentiation cultures are likely due to heterogeneous cell growth and frequency.

Interestingly, a decreased frequency of CFU-EryP in the $V^+$ fraction corresponded with the onset of the second *Gata2* expression wave at days 10–11 that is accompanied by expression of adult globin and the appearance of EMPs (Figure 2F). Thus, the *Gata2* expression peaks discriminate functional primitive and definitive stages in the ESC differentiation. It is likely that these waves derive from independent cohorts of cells as supported by transcriptomic (Scialdone et al., 2016) and hESC differentiation data (Ditadi et al., 2015; Sturgeon et al., 2014), but contrasts with data suggesting that all waves of hematopoietic activity and *in vivo* repopulating cells arise as early as day 3 (Pearson et al., 2015). Additionally, the temporal dynamics of Gata2-defined primitive/definitive stages are consistent with studies reporting hemogenic endothelium and hematopoietic cell generation in mouse ESC and hESC differentiation cultures (Nakano et al., 1996; Ng et al., 2016; Zambidis et al., 2005). Although all CFU-Cs were obtained in the $V^+$ cell fraction, FACS analysis revealed some phenotypic HPCs in the $V^-$ fraction. Hence, we cannot rule out that some early HPCs may be at low frequency in the $V^-$ fraction as was found *in vivo* (Kaimakis et al., 2016).

Morphological observation of $V^+$ cells in the differentiating EBs corroborates both developmental and functional stage changes. Day-12 (but not day-6) EBs show $CD31^+$ cells lining vascular tubules and the close association of clusters of $V^+CD31^+$ cells, mainly near the EB cavities (Figures 2E and 2E′). This is supported by FACS data showing an increased frequency of $C\text{-}KIT^+CD31^+V^+$ cells after day 6 (Figure 3D). Most probably it represents the EHT detected in E8.25–11 circulation-deficient YS where EMPs emerge in $C\text{-}KIT^+$ cell clusters (Frame et al., 2016). Although a recent study with day-23 to -33 differentiated hESCs showed similar aortic and cluster-like structures (Ng et al., 2016), it as yet uncertain, due to the heterogeneity of our cultures, whether they contain the $CD31^+V^+$ aortic endothelial and $CD31^+C\text{-}KIT^+V^+$ intra-aortic hematopoietic cluster cells equivalent to E10.5 *G2V* AGM tissue (Kaimakis et al., 2016).

Surface marker analysis of *G2V* ESC-derived cells revealed that the highest frequency of phenotypic $V^+C\text{-}KIT^+CD41^+$ hematopoietic cells is at day 8, whereas $V^+C\text{-}KIT^+CD45^+$, $V^+C\text{-}KIT^+CD16/32^+$, and $V^+C\text{-}KIT^+CD31^+$ cells peak at day 10 (Figure 3D). Thereafter their frequency is greatly reduced. These dynamics may reflect early stages of myeloid differentiation. However, our FACS data (not shown) indicate that the differentiated blood cells are within the $V^-$ cell compartment, supporting the view that the $V^+$ cell waves reflect different progenitor emergence stages. This is in line with several hESC expression profiling and surface marker studies that suggest waves of hematopoietic generation followed by blood cell maturation (Irion et al., 2010; Nakano et al., 1996; Zambidis et al., 2005). Thus, the second wave of ESC $V^+$ hematopoietic cell production functionally, morphologically, and phenotypically resembles *in vivo* definitive hematogenesis in the YS.

HPC potential in our ESC differentiation cultures continues at day 12 and thereafter, and *LG* reporter expression identifies all definitive HPCs at these late time points. LG did not enrich for primitive stage blast-cell progenitors, nor for HPCs during the first stage of EB differentiation (e.g., days 6–10). This contrasts with *G2V* ESCs where all HPCs are $V^+$ throughout the differentiation. From day 12 onward, HPC activity is significantly enriched in $G^+$ fraction, and at day 14 some $G^+$ cells possess B-lymphoid potential. Distribution of HPC activity in the *LG* EBs is consistent with the distribution in the *LG* mouse embryos. In the *LG* YS, most HPCs are $G^-$ whereas AGM lymphoid progenitors at E10 and multipotent HPCs/HSC are at much higher frequency in the E10.5/11.5 $G^+$ than in the $G^-$ fraction (de Bruijn et al., 2002; Li et al., 2014; Solaimani Kartalaei et al., 2015). In the E10.5 aorta, *LG* expression reports hemogenic endothelial cells transitioning to HSCs (Boisset et al., 2010). Thus, *LG* expression *in vivo* specifically reports aortic HSCs and cells with lymphoid potential, but not the YS-stage progenitors. Although there is consistency between our *in vitro LG* ESC results and *in vivo LG* mouse data, it is as yet uncertain whether the ESC-derived definitive $G^+$ progenitors that have B-lymphoid potential represent an aorta-like or YS-definitive program, as lymphoid potential has also

been demonstrated in the YS independently from arterial identity (Frame et al., 2016; Yoshimoto et al., 2011).

Importantly, our *LGGV* double reporter ESC line shows that these late $G^+$ HPC co-express Gata2, thus facilitating high enrichment of multipotent progenitors that are generated in late ESC differentiation cultures. In some preliminary short-term transplantation experiments ($4 \times 10^4$ $V^+$ cells from day-12 or -14 differentiated *G2V* ESCs) we were unable to detect donor-derived spleen colonies. Such short-term and long-term transplantation experiments with the *LGGV* ESC line are planned after further optimization of the differentiation cultures and flow-cytometric enrichment.

In conclusion, we demonstrate that different stages of HPC generation can be prospectively isolated by the *G2V* and/or *LG* reporter expression in ESC differentiation cultures. Such findings facilitate a better understanding of the hematopoietic development in ESC differentiation cultures, and should ultimately enable the recapitulation of robust physiologic HSC emergence for the *de novo* generation of transplantable HSCs.

## EXPERIMENTAL PROCEDURES

### ESC *In Vitro* Differentiation

ESCs (WT, *G2V*, *LG*, *LGGV*) were established from 129/Ola, *Gata2Venus* (Kaimakis et al., 2016), *Ly6a*(SCA1)*GFP* (de Bruijn et al., 2002), and (*Gata2Venus* × *Ly6a*(SCA1)*GFP*)F1 day-3.5 blastocysts cultured on irradiated mouse embryonic fibroblasts (MEFs) in SR-ES medium (KO DMEM + 20% KO Serum Replacement + 1% penicillin/streptomycin [P/S] + 2 mM L-glutamine + 1× non-essential amino acids [NEAA] [all Gibco] + 100 mM β-mercaptoethanol [Sigma] + recombinant mouse leukemia inhibitory factor [LIF; 1,000 U/mL; Chemicon International]). To allow for inner cell mass expansion the medium was changed every 2 days and cells were trypsinized, transferred to 12-well MEF-coated plates, and maintained in DMEM (Lonza) + 15% fetal bovine serum (FBS; HyClone) + 2 mM GlutaMAX + 1 mM Na-pyruvate + 1% P/S + 50 μM β-mercaptoethanol (all Gibco) + 0.1 mM NEAA (Lonza) + 1,000 U/mL LIF (Sigma) at 37°C and 5% $CO_2$. MEFs were depleted by 30-min incubation in EB medium (Iscove's modified Dulbecco's medium [IMDM] + 15% fetal calf serum [HyClone] + 1% P/S [Gibco]). EB formation was induced (40 rpm; $25 \times 10^3$ cells/mL) in EB medium + 2 mM GlutaMAX (Gibco) + 50 μg/mL ascorbic acid (Sigma) + $4 \times 10^{-4}$ M monothioglycerol (Sigma) + 300 μg/mL transferrin (Roche) and supplemented with 5% proteome-free hybridoma medium (Gibco) on day 3. From day 6 onward, 100 ng/mL stem cell factor (SCF) + 1 ng/mL interleukin-3 (IL-3) + 5 ng/mL IL-11 were added. For blast-cell cultures, 5 ng/mL BMP4 was added on days 0–3. All factors were from PeproTech.

### FACS

PBS-washed EBs were incubated (37°C, 3–5 min) in TrypLE Express (Gibco). PBS + 10% FBS + 1% P/S was added and single cells suspended (P1000 pipette). $10^6$ cells per 100 μL were immunostained (30 min on ice) (Table S1). Dead cells were Hoechst 33342 (Invitrogen) excluded. LSRFortessa, FACScan, FACSAria III/Fusion (Becton Dickinson) and FlowJo software (TreeStar) were used. Strategy for detection of GFP and/or Venus is described in Supplemental Experimental Procedures and Figure S6.

### CFU-C Assays

For BL-CFC, day-3 EB cells were plated in methylcellulose (STEMCELL Technologies) + 10% FCS + vascular endothelial growth factor (5 ng/mL) + IL-6 (10 ng/mL) (PeproTech). After 4 days, BL-CFC (grape-like multicellular structures [Kennedy et al., 2007]) were microscopically counted. D6-14 EB cells were plated in methylcellulose (1 mL/dish, M3434; STEMCELL Technologies) + IMDM + FBS + BSA + recombinant human insulin + human transferrin (iron-saturated) + 2-mercaptoethanol + recombinant SCF + recombinant IL-3 + recombinant IL-6 + recombinant human erythropoietin. After 12–14 days, colonies were scored (Zeiss Axiovert25).

### Matrigel Assay

Day-4 EB cells ($2 \times 10^4$) from each FLK1/Venus fraction (Figure 1B) were pre-cultured in gelatin-coated 96-well plates (DMEM + 20% FBS + 1% P/S; 20 hr). Cells were trypsinized, transferred to Matrigel-coated (60 μL Matrigel/well, 30 min, 37°C; Qiagen) 96-well plates and cultured in EGM-2 (Lonza) for 4 hr. Tubules were quantified by the Angiogenesis Analyzer (Gilles Carpentier ImageJ News, 2012) plugin for Fiji.

### Transcription Analysis

Up to $10^6$ cells were lysed and total RNA isolated (TRI-Reagent, MRC). RNA (1 μg) was DNase (Invitrogen) treated. RNA from sorted cells was isolated using an RNeasy kit (Qiagen). cDNA was synthesized with oligo(dT) (Invitrogen) and SuperScriptIII (Life Technologies). qRT-PCR was performed with FastSybrGreen master mix (Life Technologies) and primers (Table S2).

### B-Lymphoid Culture

At day 6 of ESC differentiation, 100 ng/mL SCF + 1 ng/mL IL-3 + 5 ng/mL IL-11 + 5 ng/mL FLT3L were added and medium replaced every other day. On day 14, EBs were dissociated and $5–10 \times 10^4$ FACS-sorted cells plated on OP9 (plated at −1 day in a 6-well plate) in 2 mL of α-minimal essential medium + 20% FBS + 1% P/S + 5 ng/mL IL-7 + 5 ng/mL FLT3L. Every 4–6 days, cells were replated on OP9 and harvested on day 22. The FACS strategy is displayed in Figure S5.

### Whole-Mount Staining

EB staining was performed as in Yokomizo et al. (2012). EBs were washed in PBS, fixed in PBS + 2% paraformaldehyde (Sigma) for 10 min, washed in PBS (×3), and dehydrated in 50% methanol + PBS and 100% methanol (10 min, ×2). EBs were rehydrated in 1:1 methanol/PBS (10 min) and 100% methanol (10 min), washed in PBS (10 min on ice), and blocked in PBS + 1% semi-skimmed milk + 0.005% Tween 20 (Sigma) (PBS-MT) + 10% BSA (Sigma) + 0.1% goat serum (4–6 hr). Antibody (Table S1) staining was performed (4°C) in PBS-MT and EBs washed in

PBS-MT (>2 hr ×3), in 100% methanol (30 s, ×4) in a fast well, cleared in 1:1 benzyl alcohol benzyl benzoate (BABB)/methanol (30 s) followed by 100% BABB, overlaid with a coverslip, and imaged (Leica SP5).

### Statistics

Unpaired Student's t test or one-way ANOVA with Bonferroni correction for multiple comparisons were used (GraphPad). Results were statistically significant at $p < 0.05$ (*$p < 0.05$, **$p < 0.01$, ***$p < 0.001$ in figures). All data are shown as mean ± SEM. n denotes the number of biological replicates.

## SUPPLEMENTAL INFORMATION

Supplemental Information includes Supplemental Experimental Procedures, seven figures, and two tables and can be found with this article online at https://doi.org/10.1016/j.stemcr.2017.11.018.

## AUTHOR CONTRIBUTIONS

M.-L.K., C.R.-S., P.K., S.C.M., X.C.-L., and U.H. designed and performed the research; S.C.M., P.K., and U.H. generated reporter cell lines; M.-L.K., C.R.-S., S.C.M., X.C.-L., and E.D. analyzed data. E.D. obtained funding and directed the study. M.-L.K. and E.D. conceived the study and wrote the paper.

## ACKNOWLEDGMENTS

We thank G. Keller for ESC guidance; A. Ditadi and R.E. Rönn for analysis advice; A. Amirnasr, M. Gabriel Salazar, and A. Maglitto for ESC culture help; M. Crisan for Matrigel; S.A. Mariani and W. Ramsay for FACS advice; I. Chambers and K. Jääger for Nanog antibody; R.v.d. Linden and QMRI Flow facility for FACS sorting; and funding support from Landsteiner Society for Blood Research (LSBR 1344-1), ZonMW-TOP (103127), NIH NIDDKK (R37 DK 054077), and ERC AdV grant (341096).

Received: December 18, 2016
Revised: November 24, 2017
Accepted: November 27, 2017
Published: December 21, 2017

## REFERENCES

Boiers, C., Carrelha, J., Lutteropp, M., Luc, S., Green, J.C., Azzoni, E., Woll, P.S., Mead, A.J., Hultquist, A., Swiers, G., et al. (2013). Lymphomyeloid contribution of an immune-restricted progenitor emerging prior to definitive hematopoietic stem cells. Cell Stem Cell *13*, 535–548.

Boisset, J.C., van Cappellen, W., Andrieu-Soler, C., Galjart, N., Dzierzak, E., and Robin, C. (2010). In vivo imaging of haematopoietic cells emerging from the mouse aortic endothelium. Nature *464*, 116–120.

Chen, M.J., Li, Y., De Obaldia, M.E., Yang, Q., Yzaguirre, A.D., Yamada-Inagawa, T., Vink, C.S., Bhandoola, A., Dzierzak, E., and Speck, N.A. (2011). Erythroid/myeloid progenitors and hematopoietic stem cells originate from distinct populations of endothelial cells. Cell Stem Cell *9*, 541–552.

Choi, K., Kennedy, M., Kazarov, A., Papadimitriou, J.C., and Keller, G. (1998). A common precursor for hematopoietic and endothelial cells. Development *125*, 725–732.

de Bruijn, M.F., Ma, X., Robin, C., Ottersbach, K., Sanchez, M.J., and Dzierzak, E. (2002). Hematopoietic stem cells localize to the endothelial cell layer in the midgestation mouse aorta. Immunity *16*, 673–683.

de Pater, E., Kaimakis, P., Vink, C.S., Yokomizo, T., Yamada-Inagawa, T., van der Linden, R., Kartalaei, P.S., Camper, S.A., Speck, N., and Dzierzak, E. (2013). Gata2 is required for HSC generation and survival. J. Exp. Med. *210*, 2843–2850.

Ditadi, A., Sturgeon, C.M., Tober, J., Awong, G., Kennedy, M., Yzaguirre, A.D., Azzola, L., Ng, E.S., Stanley, E.G., French, D.L., et al. (2015). Human definitive haemogenic endothelium and arterial vascular endothelium represent distinct lineages. Nat. Cell Biol. *17*, 580–591.

Doetschman, T.C., Eistetter, H., Katz, M., Schmidt, W., and Kemler, R. (1985). The in vitro development of blastocyst-derived embryonic stem cell lines: formation of visceral yolk sac, blood islands and myocardium. J. Embryol. Exp. Morphol. *87*, 27–45.

Doulatov, S., Vo, L.T., Chou, S.S., Kim, P.G., Arora, N., Li, H., Hadland, B.K., Bernstein, I.D., Collins, J.J., Zon, L.I., et al. (2013). Induction of multipotential hematopoietic progenitors from human pluripotent stem cells via respecification of lineage-restricted precursors. Cell Stem Cell *13*, 459–470.

Dzierzak, E., and Speck, N.A. (2008). Of lineage and legacy: the development of mammalian hematopoietic stem cells. Nat. Immunol. *9*, 129–136.

Eich, C., Arlt, J., Vink, C.S., Solaimani Kartalaei, P., Kaimakis, P., Mariani, S., van der Linden, R., van Cappelen, W.A., and Dzierzak, E. (2017). In vivo single cell analysis reveals Gata2 dynamics in cells transitioning to hematopoietic fate. J. Exp. Med. https://doi.org/10.1084/jem.20170807.

Frame, J.M., Fegan, K.H., Conway, S.J., McGrath, K.E., and Palis, J. (2016). Definitive hematopoiesis in the yolk sac emerges from Wnt-responsive hemogenic endothelium independently of circulation and arterial identity. Stem Cells *34*, 431–444.

Frame, J.M., McGrath, K.E., and Palis, J. (2013). Erythro-myeloid progenitors: "definitive" hematopoiesis in the conceptus prior to the emergence of hematopoietic stem cells. Blood Cells Mol. Dis. *51*, 220–225.

Gao, X., Johnson, K.D., Chang, Y.I., Boyer, M.E., Dewey, C.N., Zhang, J., and Bresnick, E.H. (2013). Gata2 cis-element is required for hematopoietic stem cell generation in the mammalian embryo. J. Exp. Med. *210*, 2833–2842.

Godin, I., Dieterlen-Lievre, F., and Cumano, A. (1995). Emergence of multipotent hemopoietic cells in the yolk sac and paraaortic splanchnopleura in mouse embryos, beginning at 8.5 days postcoitus. Proc. Natl. Acad. Sci. USA *92*, 773–777.

Huang, K., Du, J., Ma, N., Liu, J., Wu, P., Dong, X., Meng, M., Wang, W., Chen, X., Shi, X., et al. (2015). GATA2(-/-) human ESCs undergo attenuated endothelial to hematopoietic transition and thereafter granulocyte commitment. Cell Regen. (Lond.) *4*, 4.

Huang, K., Gao, J., Du, J., Ma, N., Zhu, Y., Wu, P., Zhang, T., Wang, W., Li, Y., Chen, Q., et al. (2016). Generation and analysis of

GATA2w/eGFP human ESCs reveal ITGB3/CD61 as a reliable marker for defining hemogenic endothelial cells during hematopoiesis. Stem Cell Reports *7*, 854–868.

Huber, T.L., Kouskoff, V., Fehling, H.J., Palis, J., and Keller, G. (2004). Haemangioblast commitment is initiated in the primitive streak of the mouse embryo. Nature *432*, 625–630.

Irion, S., Clarke, R.L., Luche, H., Kim, I., Morrison, S.J., Fehling, H.J., and Keller, G.M. (2010). Temporal specification of blood progenitors from mouse embryonic stem cells and induced pluripotent stem cells. Development *137*, 2829–2839.

Kaimakis, P., de Pater, E., Eich, C., Solaimani Kartalaei, P., Kauts, M.L., Vink, C.S., van der Linden, R., Jaegle, M., Yokomizo, T., Meijer, D., et al. (2016). Functional and molecular characterization of mouse Gata2-independent hematopoietic progenitors. Blood *127*, 1426–1437.

Katsumura, K.R., Bresnick, E.H., and Group, G.F.M. (2017). The GATA factor revolution in hematology. Blood *129*, 2092–2102.

Kauts, M.L., Vink, C.S., and Dzierzak, E. (2016). Hematopoietic (stem) cell development—how divergent are the roads taken? FEBS Lett. *590*, 3975–3986.

Kennedy, M., Firpo, M., Choi, K., Wall, C., Robertson, S., Kabrun, N., and Keller, G. (1997). A common precursor for primitive erythropoiesis and definitive haematopoiesis. Nature *386*, 488–493.

Kennedy, M., D'Souza, S.L., Lynch-Kattman, M., Schwantz, S., and Keller, G. (2007). Development of the hemangioblast defines the onset of hematopoiesis in human ES cell differentiation cultures. Blood *109*, 2679–2687.

Kennedy, M., Awong, G., Sturgeon, C.M., Ditadi, A., LaMotte-Mohs, R., Zuniga-Pflucker, J.C., and Keller, G. (2012). T lymphocyte potential marks the emergence of definitive hematopoietic progenitors in human pluripotent stem cell differentiation cultures. Cell Rep. *2*, 1722–1735.

Kingsley, P.D., Malik, J., Emerson, R.L., Bushnell, T.P., McGrath, K.E., Bloedorn, L.A., Bulger, M., and Palis, J. (2006). "Maturational" globin switching in primary primitive erythroid cells. Blood *107*, 1665–1672.

Lancrin, C., Sroczynska, P., Stephenson, C., Allen, T., Kouskoff, V., and Lacaud, G. (2009). The haemangioblast generates haematopoietic cells through a haemogenic endothelium stage. Nature *457*, 892–895.

Li, Y., Esain, V., Teng, L., Xu, J., Kwan, W., Frost, I.M., Yzaguirre, A.D., Cai, X., Cortes, M., Maijenburg, M.W., et al. (2014). Inflammatory signaling regulates embryonic hematopoietic stem and progenitor cell production. Genes Dev. *28*, 2597–2612.

Ling, K.W., Ottersbach, K., van Hamburg, J.P., Oziemlak, A., Tsai, F.Y., Orkin, S.H., Ploemacher, R., Hendriks, R.W., and Dzierzak, E. (2004). GATA-2 plays two functionally distinct roles during the ontogeny of hematopoietic stem cells. J. Exp. Med. *200*, 871–882.

Lis, R., Karrasch, C.C., Poulos, M.G., Kunar, B., Redmond, D., Duran, J.G.B., Badwe, C.R., Schachterle, W., Ginsberg, M., Xiang, J., et al. (2017). Conversion of adult endothelium to immunocompetent haematopoietic stem cells. Nature *545*, 439–445.

Mascarenhas, M.I., Parker, A., Dzierzak, E., and Ottersbach, K. (2009). Identification of novel regulators of hematopoietic stem cell development through refinement of stem cell localization and expression profiling. Blood *114*, 4645–4653.

Medvinsky, A., and Dzierzak, E. (1996). Definitive hematopoiesis is autonomously initiated by the AGM region. Cell *86*, 897–906.

Minegishi, N., Ohta, J., Yamagiwa, H., Suzuki, N., Kawauchi, S., Zhou, Y., Takahashi, S., Hayashi, N., Engel, J.D., and Yamamoto, M. (1999). The mouse GATA-2 gene is expressed in the para-aortic splanchnopleura and aorta-gonads and mesonephros region. Blood *93*, 4196–4207.

Muller, A.M., Medvinsky, A., Strouboulis, J., Grosveld, F., and Dzierzak, E. (1994). Development of hematopoietic stem cell activity in the mouse embryo. Immunity *1*, 291–301.

Nakano, T., Kodama, H., and Honjo, T. (1996). In vitro development of primitive and definitive erythrocytes from different precursors. Science *272*, 722–724.

Ng, E.S., Azzola, L., Bruveris, F.F., Calvanese, V., Phipson, B., Vlahos, K., Hirst, C., Jokubaitis, V.J., Yu, Q.C., Maksimovic, J., et al. (2016). Differentiation of human embryonic stem cells to HOXA+ hemogenic vasculature that resembles the aorta-gonad-mesonephros. Nat. Biotechnol. *34*, 1168–1179.

Palis, J., Malik, J., McGrath, K.E., and Kingsley, P.D. (2010). Primitive erythropoiesis in the mammalian embryo. Int. J. Dev. Biol. *54*, 1011–1018.

Palis, J., Robertson, S., Kennedy, M., Wall, C., and Keller, G. (1999). Development of erythroid and myeloid progenitors in the yolk sac and embryo proper of the mouse. Development *126*, 5073–5084.

Pearson, S., Cuvertino, S., Fleury, M., Lacaud, G., and Kouskoff, V. (2015). In vivo repopulating activity emerges at the onset of hematopoietic specification during embryonic stem cell differentiation. Stem Cell Reports *4*, 431–444.

Robert-Moreno, A., Espinosa, L., de la Pompa, J.L., and Bigas, A. (2005). RBPjkappa-dependent Notch function regulates Gata2 and is essential for the formation of intra-embryonic hematopoietic cells. Development *132*, 1117–1126.

Robin, C., Ottersbach, K., Boisset, J.C., Oziemlak, A., and Dzierzak, E. (2011). CD41 is developmentally regulated and differentially expressed on mouse hematopoietic stem cells. Blood *117*, 5088–5091.

Rodrigues, N.P., Janzen, V., Forkert, R., Dombkowski, D.M., Boyd, A.S., Orkin, S.H., Enver, T., Vyas, P., and Scadden, D.T. (2005). Haploinsufficiency of GATA-2 perturbs adult hematopoietic stem-cell homeostasis. Blood *106*, 477–484.

Sankaran, V.G., Xu, J., and Orkin, S.H. (2010). Advances in the understanding of haemoglobin switching. Br. J. Haematol. *149*, 181–194.

Scialdone, A., Tanaka, Y., Jawaid, W., Moignard, V., Wilson, N.K., Macaulay, I.C., Marioni, J.C., and Gottgens, B. (2016). Resolving early mesoderm diversification through single-cell expression profiling. Nature *535*, 289–293.

Shalaby, F., Ho, J., Stanford, W.L., Fischer, K.D., Schuh, A.C., Schwartz, L., Bernstein, A., and Rossant, J. (1997). A requirement for Flk1 in primitive and definitive hematopoiesis and vasculogenesis. Cell *89*, 981–990.

Solaimani Kartalaei, P., Yamada-Inagawa, T., Vink, C.S., de Pater, E., van der Linden, R., Marks-Bluth, J., van der Sloot, A., van den Hout, M., Yokomizo, T., van Schaick-Solerno, M.L., et al. (2015). Whole-transcriptome analysis of endothelial to hematopoietic stem cell

transition reveals a requirement for Gpr56 in HSC generation. J. Exp. Med. *212*, 93–106.

Sturgeon, C.M., Ditadi, A., Awong, G., Kennedy, M., and Keller, G. (2014). Wnt signaling controls the specification of definitive and primitive hematopoiesis from human pluripotent stem cells. Nat. Biotechnol. *32*, 554–561.

Sugimura, R., Jha, D.K., Han, A., Soria-Valles, C., da Rocha, E.L., Lu, Y.F., Goettel, J.A., Serrao, E., Rowe, R.G., Malleshaiah, M., et al. (2017). Haematopoietic stem and progenitor cells from human pluripotent stem cells. Nature *545*, 432–438.

Tsai, F.Y., Keller, G., Kuo, F.C., Weiss, M., Chen, J., Rosenblatt, M., Alt, F.W., and Orkin, S.H. (1994). An early haematopoietic defect in mice lacking the transcription factor GATA-2. Nature *371*, 221–226.

Wilson, N.K., Foster, S.D., Wang, X., Knezevic, K., Schutte, J., Kaimakis, P., Chilarska, P.M., Kinston, S., Ouwehand, W.H., Dzierzak, E., et al. (2010). Combinatorial transcriptional control in blood stem/progenitor cells: genome-wide analysis of ten major transcriptional regulators. Cell Stem Cell *7*, 532–544.

Yoder, M.C., Hiatt, K., Dutt, P., Mukherjee, P., Bodine, D.M., and Orlic, D. (1997). Characterization of definitive lymphohematopoietic stem cells in the day 9 murine yolk sac. Immunity *7*, 335–344.

Yokomizo, T., Yamada-Inagawa, T., Yzaguirre, A.D., Chen, M.J., Speck, N.A., and Dzierzak, E. (2012). Whole-mount three-dimensional imaging of internally localized immunostained cells within mouse embryos. Nat. Protoc. *7*, 421–431.

Yoshimoto, M., Montecino-Rodriguez, E., Ferkowicz, M.J., Porayette, P., Shelley, W.C., Conway, S.J., Dorshkind, K., and Yoder, M.C. (2011). Embryonic day 9 yolk sac and intra-embryonic hemogenic endothelium independently generate a B-1 and marginal zone progenitor lacking B-2 potential. Proc. Natl. Acad. Sci. USA *108*, 1468–1473.

Zambidis, E.T., Peault, B., Park, T.S., Bunz, F., and Civin, C.I. (2005). Hematopoietic differentiation of human embryonic stem cells progresses through sequential hematoendothelial, primitive, and definitive stages resembling human yolk sac development. Blood *106*, 860–870.